*32nd EPS Conference on Plasma Phys. Tarragona, 27 June - 1 July 2005 ECA Vol.**29C**, P-5.006 (2005)*

ELM propagation and fluctuations in SOL and divertor on JT-60U Tokamak

N. Asakura[1], M. Takechi[1], G. Matshunaga[1], N. Oyama[1], T. Nakano[1],
H. Miyoshi[2], N. Ohno[3], S. Takamura[2], Y. Uesugi[4]
[1]*Japan Atomic Energy Research Institute, Naka, Ibaraki 311-0193, Japan*
[2]*Department of Energy Engineering and Science, Graduate School of Engineering, Nagoya Univ, Nagoya, Japan*
[3]*EcoTopia Science Research Institute, Nagoya Univ., Nagoya 464-8603, Japan*
[4]*Department of Electrical and Electronic Engineering, Kanazawa Univ. Kanazawa 920-8667, Japan*

1. Introduction

Transient heat and particle loading caused by Edge Localized Mode (ELM) is crucial for determining the lifetime of ITER divertor materials. At the same time, radial transport of ELM plasma should be understood to determinethe heat and particle fluxes to the first wall. Parallel and radial propagation of the ELM plasma has been investigated [1], using reciprocating Mach probes (at Low-Field-Side midplane and X-point), target probes and magnetic pick-up coils at the first wall. The sampling rate was recently improved from 200 to 500 kHz. Multi peaks in waveform of ion saturation current of the midplane probe, j_s^{mid}, were identified during ELM event, and time and amplitude of ELM bursts were determined.

Dynamics of diffusion is a fundamental problem in the SOL study. In particular, SOL density at outer flux surfaces (far SOL) was increased in high density discharges [2]. Enhancement of particle flux at far SOL as well as ELM plasma flux increases the main chamber recycling, potentially causing the density control less efficient. Recently, turbulence and non-diffusive transport models are of great interest to understand the radial transport. Characteristics of the fluctuations in j_s^{mid} are investigated in L- and ELMy H-modes.

2. ELM transport to the divertor

ELM plasma propagation was investigated in Type-I ELMy H-mode (I_p=1MA, B_t=2T, δ=0.32, κ=1.4, P_{NB}= 4.3MW, $\bar{n}_e$=1.7x10^{19} m^{-3}). ELM frequency was 20-30Hz, and 10-15 ELMs were measured at the different radius during an insertion of the Mach probe. Figure 1 shows rapid change in magnetic fluctuations ($\tilde{B}_p$), j_s^{div}, D_α brightness and heat flux near the High-Field-Side and LFS strike-points. Here, locations of strike-points are between two target probes, i.e. P8-P9 and P10-P11, where separation of the two probe is 3 cm. At ELM

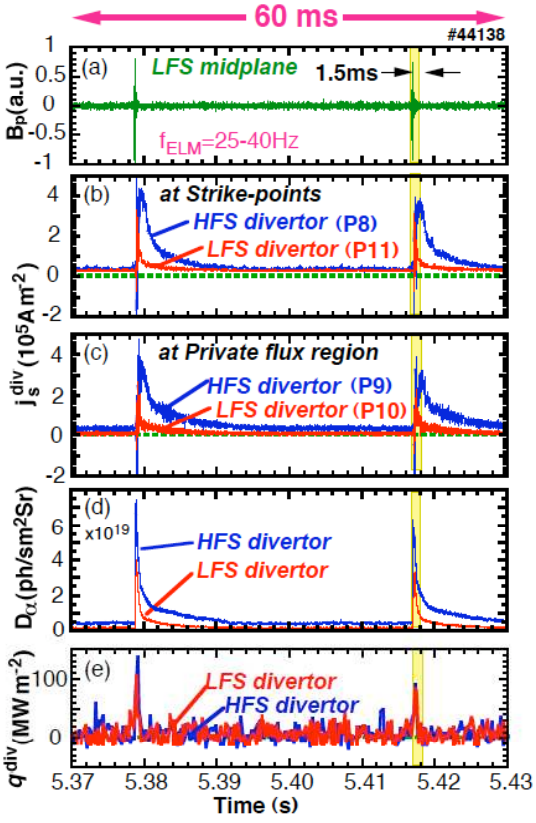

Fig.1 (a) Magnetic fluctuations, (b) j_s at LFS&HFS strike-points, (c) j_s at LFS&HFS private region, (d) D_α brightness, (e) peak heat flux near LFS&HFS strike-points,.

event, j_s^{div} is increased largely even at the private region. After the ELM event, decay times of j_s^{div} and D_α brightness are comparable. Deposition of the heat flux is short (corresponding to one frame of IRTV, 250μs). Rapid change of the divertor plasma is investigated.

Figure 2 shows $\tilde{B}_p$, j_s^{mid} at up-stream and down-stream sides of the Mach probe (midplane radius, Δr^{mid} is 4.8cm), j_s^{div} at the LFS strike-point and D_a brightness during the second ELM in Fig. 1 (t~5.417s). $\tilde{B}_p$ is increased at t_0^{MHD} =5416.965 ms after a short precauser. After j_s^{mid} fluctuations, i.e. large positive and negative j_s^{mid} oscillations, multi-peaks of j_s^{mid} appear. At the same time, j_s^{mid} base-level is increased. Start of the first j_s^{mid} peak after the large fluctuations is defined as delay due to the SOL plasma transport across the magnetic flield: τ_{perp}^{mid} ~40μs. Start of D_α brightness enhancement is also delayed by ~40μs, which is simultaneously at main and divertor.

After t_0^{MHD}, fluctuations in j_s^{div} are observed near the strike-point (distance from the strike-point corresponds to Δr^{mid} = 0.3cm). Then, j_s^{div} base level starts to increase after t = 5417.080 ms, and the divertor D_α brightness becomes large. Thus, the delay from t_0^{MHD}, i.e. τ_{para}^{div} = 115 μs, is defined as start of the ELM particle deposition, i.e. parallel convective transport along the magnetic field lines. As a result, the radial transport of the peak j_s^{mid} is faster than τ_{para}^{div}.

Maximum values of j_s^{div} and the divertor D_α brightness are observed ~220μs after t_0^{MHD}: the delay is defined as $\tau_{para}^{div\text{-}peak}$. Here, divertor plasma density is largely increased since neutrals are desorbed from the divetor tile surface as well as increase of plasma flux to the divertor.

Statistical ambiguities of τ_{para}^{div} and $\tau_{para}^{div\text{-}peak}$ are shown in Fig. 3 for 26 ELM events. Distribution of τ_{para}^{div} is due to variations of the transient plasma distribution, which may be caused by the toroidal and poloidal asymmetries of the ELM activity. About 70% of ELM events are observed in τ_{para}^{div} = 70-130μs and $\tau_{para}^{div\text{-}peak}$ = 130-200μs. Here, plasma convection time is $\tau_{para}^{SOL\text{-}LFS}$ =140 μs, which is between τ_{para}^{div} and $\tau_{para}^{div\text{-}peak}$. This result is similar to the previous result with

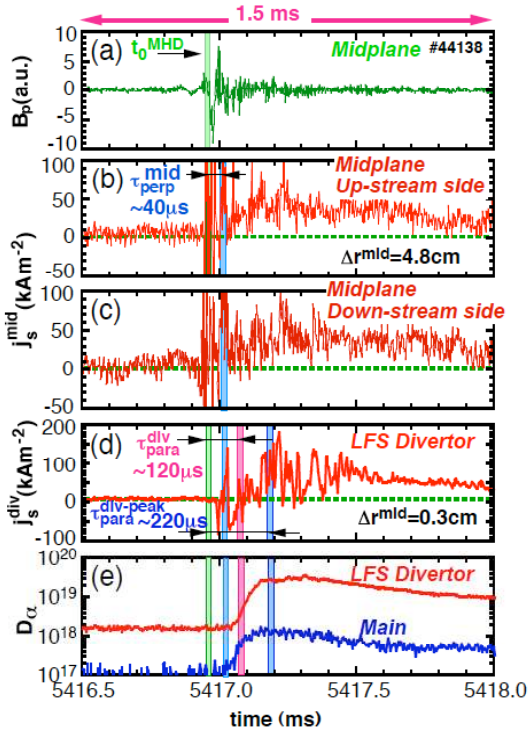

Fig.2 (a) Magnetic fluctuations, midplane j_s (b) at up-stream side and (c) at down-stream side, (d) j_s at LFS divertor, (e) D_α brightness.

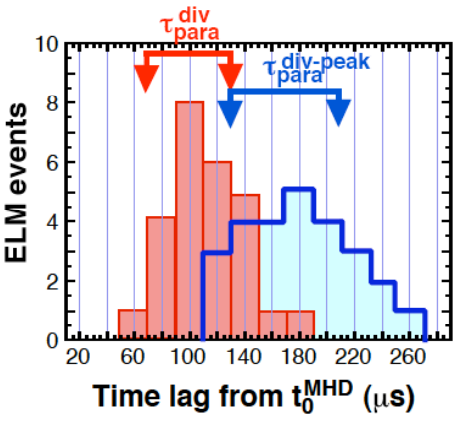

Fig.3 Distributions of time lags from t_o^{MHD} to start of j_s^{div} (τ_{para}^{div}) and j_s^{div} peak ($\tau_{para}^{div\text{-}peak}$). Thick arrows show time ranges where 70% of ELM events occur.

200kHz sampling rate [1]: τ_{para}^{div} = 70-130μs and $\tau_{para}^{div\text{-}peak}$ =150-190 μs.

3. ELM propagation to the wall

Radial propagation of the ELM plasma was investigated. Figure 4 shows time evolutions of $\tilde{B}_p$ and j_s^{mid} at Δr^{mid} = 4.8 cm. Multi-peaks appear in j_s^{mid} after large $\tilde{B}_p$ activity, and durations of three j_s^{mid} peaks are δt^{peak}=22, 10, 8 μs. Time lag of the first j_s^{mid} peak and maximum base-level are defined as τ_{perp}^{mid}(peak) and τ_{perp}^{mid}(base), respectively.

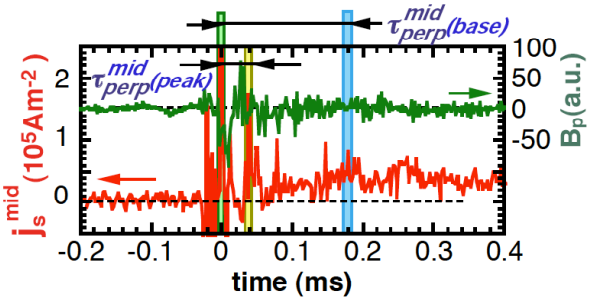

Fig.4 Time evolutions of j_s^{mid} at Δr^{mid} =4.8cm and B_p as a function of time lag from t^{MHD}.

Figure 5 shows radial profiles of the j_s^{mid} peaks (closed circles) and maximum base-levels (squares), where distance of the first wall is 21 cm. The distribution of j_s^{mid}(peak) is *an envelope of* j_s^{mid} *peaks* rather than a profile at one moment. Enhancement factor of j_s^{mid}(peak) compared to j_s^{mid} base-level between ELMs (open circles) is 10-20 over a wide SOL region. On the other hand, increment of j_s^{mid}(base) is small (2-6 times), and it is observed at Δr^{mid} < 10 cm.

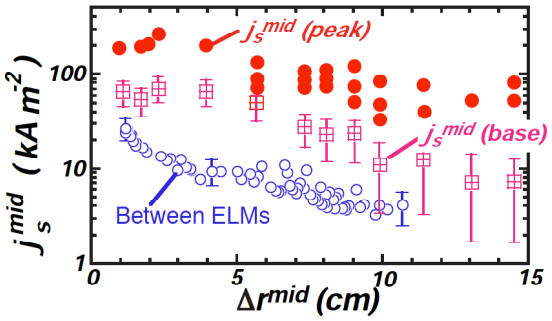

Fig.5 Distributions of j_s^{mid} peaks (closed circle), maximum base-level (square) during ELM, and j_s^{mid} between ELMs

Radial propagation velocities of j_s^{mid}(peak) and j_s^{mid}(base) are evaluated from $V_{perp}^{mid} = \Delta r^{mid}/\tau_{perp}^{mid}$. Figure 6 shows τ_{perp}^{mid}(peak) and τ_{perp}^{mid}(base) as a function of Δr^{mid}. Since τ_{perp}^{mid}(peak) increases with Δr^{mid}, V_{perp}^{mid}(peak) ranges between 1.3 and 2.5 km/s, where V_{perp}^{mid}(peak) may be large at Δr^{mid} > 10 cm. From V_{perp}^{mid}~1.9km/s, radial scale of j_s^{mid} peak is estimated to $\delta t^{peak} V_{perp}^{mid}$ = 1.5 - 4cm.

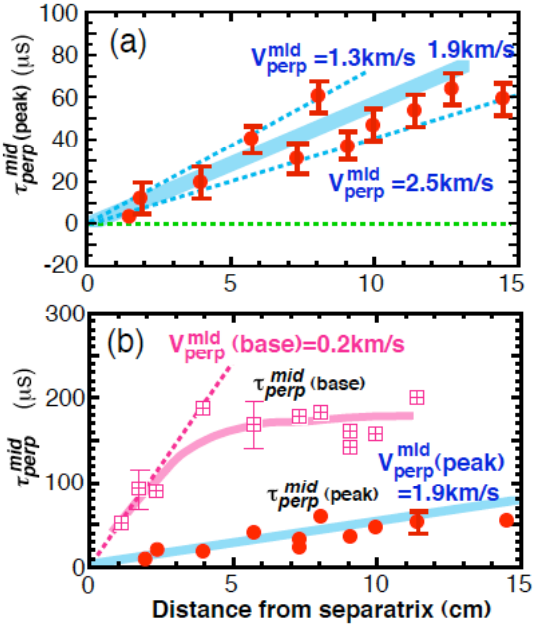

Fig.6 Distributions of τ_{perp}^{mid}(peak) and τ_{perp}^{mid}(base) are shown by closed-circles and squares, respectively.

τ_{perp}^{mid}(base) is increased with Δr^{mid} near separatrix (Δr^{mid} <4cm), and radial propagation with V_{perp}^{mid}(base) ~0.2 km/s. On the other hand, τ_{perp}^{mid}(base) is constant (150-200 μs) at far SOL, and plasma propagation is not identified. Here the time lag is comparable to that at the divertor ($\tau_{para}^{div\text{-}peak}$ = 130-200 μs). Such such time scale is comparable to neutral transport with relatively high energy of 10-20 eV, neutral recycling may be a candidate.

4. Fluctuations in ELMy H- and L-mode SOLs

Fluctuation levels, $\delta j_s/\langle j_s\rangle$, in j_s^{mid} and j_s^{Xp} were compared in L-mode and ELMy H-mode plasmas. For the L-mode case, B_t = 2.7T was higher and $\bar{n}_e$=1.4x10^{19} m^{-3} was lower than those for ELMy H-mode. Gas puff was not injected during the measurement. Here, δj_s and $\langle j_s\rangle$ are R.M.S. and average values of j_s during 1 ms. During ELM event, $\langle j_s\rangle$ corresponds to j_s^{mid}(base) rather than j_s^{mid}(peak).

Profiles of $\langle j_s^{mid}\rangle$ and $\delta j_s^{mid}/\langle j_s^{mid}\rangle$ for the ELMy H- and L-modes are shown in Fig. 7. e-folding lengths of two profiles are similar (3-4 cm), but $\langle j_s^{mid}\rangle$ for ELMy-H mode is about 1/5 of $\langle j_s^{mid}\rangle$ for L-mode. During ELM activity, $\langle j_s^{mid}\rangle$ is enhanced up to $\langle j_s^{mid}\rangle$ for L-mode. Near the separatrix (Δr^{mid} < 3 cm), two values of $\delta j_s^{mid}/\langle j_s^{mid}\rangle$ (0.4-0.5 for H-mode and 0.3-0.4 for L-mode) are comparable. On the other hand, at far SOL (Δr^{mid} > 3 cm), $\delta j_s^{mid}/\langle j_s^{mid}\rangle$ for ELMy H-mode becomes large (a factor of 5-10).

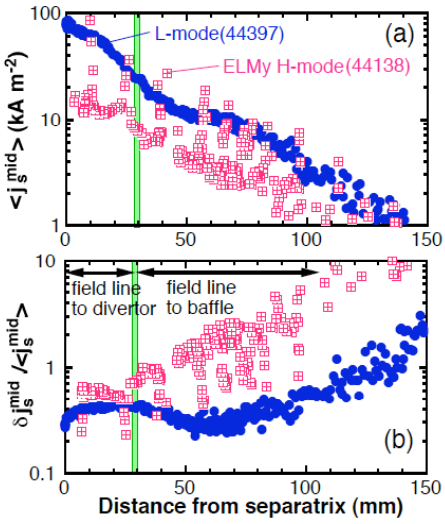

Fig.7 Profiles in ELMy H- and L-modes: (a) ion saturation current at midplane, (b) the fluctuation level.

Profiles of $\langle j_s^{Xp}\rangle$ and $\delta j_s^{Xp}/\langle j_s^{Xp}\rangle$ for the ELMy H- and L-modes are compared in Fig.8, where corresponding midplane radius of the divertor region is 3.2 cm. $\langle j_s^{Xp}\rangle$ between ELMs is 10 times smaller than $\langle j_s^{Xp}\rangle$ in L-mode, while $\langle j_s^{Xp}\rangle$ is enhanced to $\langle j_s^{Xp}\rangle$ in L-mode. Both for ELMy H- and L-mode cases, $\delta j_s^{Xp}/\langle j_s^{Xp}\rangle$ are 4-5 times smaller than those at midplane: it is found that fluctuation level at LFS SOL is generally large compared to that near X-point.

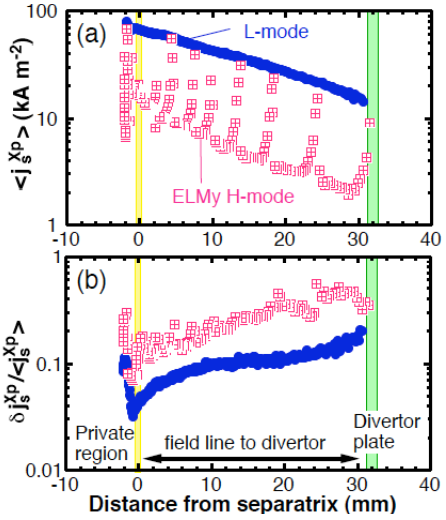

Fig.8 Profiles in ELMy H- and L-modes: (a) ion saturation current at X-point, (b) the fluctuation level.

5. Summary

Parallel and radial ELM transport was investigated in SOL and divertor. Two characteristics in j_s^{mid} enhancement were observed. (1) Large multi-peaks in j_s^{mid} were observed over all radii (Δr^{mid} < 15 cm), and the radial velocity with variation of 1.3 and 2.5 km/s was determined. Propagation towards the first wall (60-80 μs) was faster than the transport time to the divertor, i.e. parallel convection (70-130 μs). (2) Enhancement of j_s^{mid} base-level occurred globally and simultaneously in far SOL and divertor, and j_s increased to the L-mode level. However, j_s^{mid} increment extended to smaller SOL radius (Δr^{mid} < 10 cm).

Fluctuation level of the midplane SOL plasma is 4-5 times large compared to that near X-point. $\delta j_s^{mid}/\langle j_s^{mid}\rangle$ in far SOL for H-mode was 5-10 times larger than that for L-mode, whereas e-folding lengths of $\langle j_s^{mid}\rangle$ profiles were comparable.

References

/1/ N.Asakura, M. Takechi, N.Oyama, et al., J. Nucl. Materials 337-339, (2005) 712.
/2/ N. Asakura et al., J. Nucl. Mater. **241-243** (1997) 559.